

Table 1: Complete list of primer sequences used for quantitative RT-PCR for all genes assessed in this study.

Fig. S1. (A) Gene expression microarray and GSEA analyses of parental MCF7^{neo} cells expressing an empty plasmid encoding the neomycin resistance cassette compared with MCF7^{10X} which expresses elevated levels of SOD2. (B) Quantification of Western blot images in Fig. 1A. (C) Quantification of Western blot images in Fig. 1B. (D) Quantitative RT-PCR for HIF2 α mRNA level in MCF7^{neo}, MCF7^{6X}, and MCF7^{10X}. Errors represent \pm SD. ** $p < 0.01$.

Fig. S2. (A) Verification of differential gene expression shown in Fig. S1 was performed by RT-QPCR in MCF7^{neo}, MCF7^{6X}, and MCF7^{10X} cells. Genes from each of the gene sets were selected randomly base only on expression levels detected using microarray analysis. * $p < 0.05$, ** $p < 0.01$, and were compared to MCF7^{neo}. CDKN2D encodes a member of INK4 family of inhibitors of cyclin-dependent kinases that has been shown to be involved in oxidative stress induced senescence. PDLIM1 is involved in assembly, disassembly and direction of stress fiber formation in fibroblasts. PFKFB3 generates fructose 1,6-bisphosphate and has key roles in the regulation of the glycolytic flow. SNAI2 encodes a member of the Snail family of C2H2-type zinc finger transcription factors which represses E-cadherin expression and contributes to EMT. TGFBI is a TGF β induced gene encoding matrix protein remodeling proteins. GLRX is a gene induced by hypoxia that encodes for glutaredoxin, an enzyme involved in glutathione recycling (B) Western blot analysis of Akt phosphorylation levels used in this experiment as a proxy of PTEN activity. (C) Western blot analysis of PTEN expression and oxidation status. Results indicate that there is not significant differences in the total PTEN protein levels or PTEN oxidation status in MCF7^{6X} and MCF7^{10X} compared to MCF7^{neo}.

Fig. S3. Representative flow cytometry plots of the SORE6⁺ (GFP⁺, cancer stem cell) subpopulation in parental MCF7^{neo} and MCF7^{10X} cell cultures.

Fig. S4. SOD2 overexpression leads to the accumulation of Ac-SOD2 and an increase in CD44⁺/CD24⁻ CSC subpopulation. Western blot analysis shows that overexpressing SOD2 in T47D (A) or in ZR75-1 (B) cells leads to upregulation of HIF2 α and an increase in the levels of SOD2-K68 acetylation. FACS analysis of CD44⁺/CD24⁻ expression on the surface of paraformaldehyde fixed cells in T47D (C) and ZR75-1 (D) cells overexpressing SOD2 (OE). N=3, errors represent \pm SD. * $P < 0.05$.

Fig. S5. (A) Quantification of Western blot images shown in Fig. 3E. (B) Effect of expressing SOD2 acetylation mimetic mutant (K68Q) on SORE6⁺ subpopulation in MCF7 breast cancer cell cultures. Stem cell population was measured by the genetically encoded SORE6/GFP transfected into MCF7 cells expressing wild type SOD2, SOD2 K68R, or SOD2 K68Q mutation. N=3. Errors represent \pm SD. * $p < 0.05$. (C) Western Blot for SOD2K68Ac, SOD2, HIF2 α in PyVT mouse tumors compared to non-carrier FVB mouse mammary glands.

Fig. S6. Ingenuity IPA pathway analysis of activated signaling pathways in MCF7 cells expressing SOD2 K68Q vs SOD2 K68R. The red or green arrows indicate the genes that are up or down regulated ($|\log_2| > 1$) in SOD2K68Q cells compared with SOD2K68R cells.

Fig. S7. Sirtuin-3 knockdown increases SOD2 K68 acetylation level and HIF2 α in MCF7 cells. (A) Western blot of SOD2^{K68Ac} and HIF2 α in MCF7 cells with Sirtuin-3 knockdown. (B) Quantification of SOD2^{K68Ac} and HIF2 α in (A). (C) Extracellular H₂O₂ accumulation was determined by Amplex Red fluorescence assay. Data were pooled from two independent experiments, N=12. Errors represent \pm SD. ** $p < 0.01$. (D) H₂O₂ generated in mitochondria was assessed using the probe 3-(Dihydroxyboronyl)Benzyltriphenylphosphonium bromide (MitoB). MitoB and the product of its reaction with H₂O₂ MitoP were quantified using LC-MS, N=4. Errors represent \pm SD. * $p < 0.05$. (E) knocking down of the mitochondrial acetyl transferase GCN5L1 leads to reduced SOD2 acetylation levels (F). (G) Quantification SOD2^{K68Ac} normalized on total SOD2 after both are normalized by B-actin in (F). Effect of GCN5L1 knockdown on the expression of Oct4 (H) and Nanog (I) mRNA expression as well as the number of SORE6⁺ cells (J). N=3. Errors represent \pm SD. * $p < 0.05$ and ** $p < 0.01$.

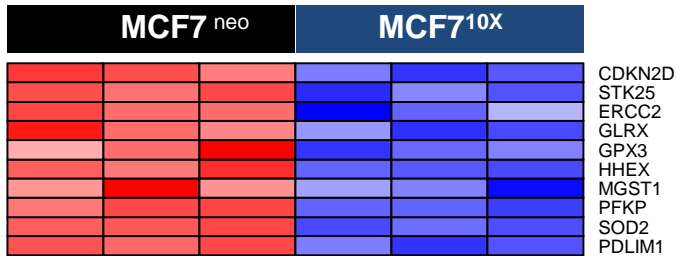
Fig. S8. (A) Catalase activity assay measured using a kit by BioVision according to the manufacturer's instructions and (B) Invasion assay (pooled two experiments, with three biological replicates each, N=6) for MCF7^{10X} cells treated with PEG-catalase or transfected with mito-catalase. (C) Colony formation assay stained with Nitroblue for MCF7^{10X} cells treated with 10 μ M of either Euk8 or Euk134 for 21 days. (D) Quantification of colonies from the experiments shown in (C), performed by counting colonies using a inverted microscope, N=6. (E) Quantification of Oct4 mRNA expression as well as (F) Nanog mRNA level by RT-QPCR in cells treated with Euk8 or Euk8 compared to controls. (G) Effect of Prx3 or (H) Gpx4 overexpression on the levels of Oct4 (I) and Nanog (J) mRNA expression. Representative of two independent experiments with 3 biologic replicates each. (K) GSH/GSSH level was measured in MCF7^{10X} cells compared to control cells. Errors represent \pm SD. *p < 0.05 and **p < 0.01.

Table 1: primer sequences used for quantitative RT-PCR

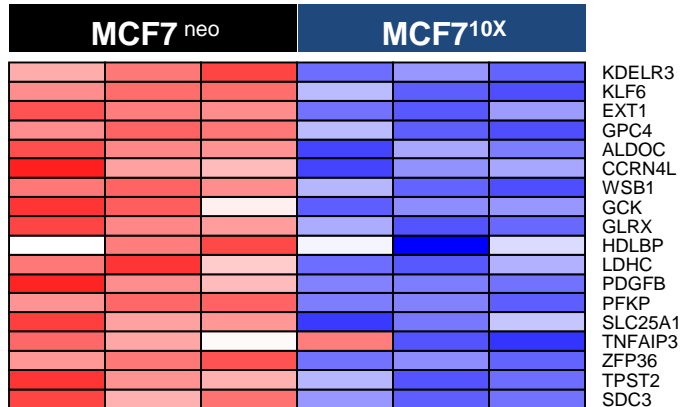
Gene names	Primer sequences
ADAM12-F	ATGGCGGTTGAGAAAGGAGG
ADAM12-R	TCTGTTCCCACACTTCTGGC
CDKND2-F	TGTCGACATGCTGCTGGAG
CDKND2-R	GGGTGTCCAGGAATCCAGTG
GAPDH-F	ATGACATCAAGAAGGTGGTGAAG
GAPDH-R	CCTGTTGCTGTAGCCAAATTC
GCN5L1-F	GTCCCGCCTCCTAAAAGAAC
GCN5L1-R	GACCTGTAGGGTCTTCACCTCAT
GLRX-F	CCTGGGAAGGTGGTTGTGTT
GLRX-R	GTGGTACTGCAGAGCTCCA
GPX4-F	GTAACCAGTTCGGGAAGCAG
GPX4-R	GGGTTGGATCTTCATCCACTT
HIF1 α F	GACTTGCCTTTCCTTCTCTTCTC
HIF1 α R	TTATGTGGAAGTGGCAACTGAT
Hif2 α -F	GGAGACGGAGGTGTTCTATGAG
Hif2 α -R	CTCCAAGGCTTTCAGGTACAAG
NANOG-F	AGATGCAAGAACTCTCCAACATC
NANOG-R	AAGAGTAAAGGCTGGGGTAGGTAG
Oct4-F	CAGTATCGAGAACCGAGTGAGAG
Oct4-R	AAAATCCTCTCGTTGTGCATAGTC
PDLIM1-F	ACCACCCAGCAGATAGACCT
PDLIM1-R	TCAAGTTGTCTGTGCAGCCT
PFKP-F	GTTCCCGCTACTGTGTCCAA
PFKP-R	GCCCATGGTCTCGATGATGA
PRDX3-F	GACATGTGAGTGCCATTCTT
PRDX3-R	CTCCATTGACAACGGCTGTA
Sirt3 F1	AAAGCCTAGTGGAGCTTCTGG
Sirt3 R1	ATTGGGATGTGGATGTCTCCTAT
SNAI2-F	AGCGAACTGGACACACATACA
SNAI2-R	ACTCACTCGCCCCAAAGATG
SOD2-F	ACCGAGGAGAAGTACCAGGAG
SOD2-R	ACTTGTCAAAGGAACCAAAGTCAC
TGFBI-F	CTCCCTGGTCAGCAATGTCA
TGFBI-R	CCGGGCACAGTTCACAGTTA

A

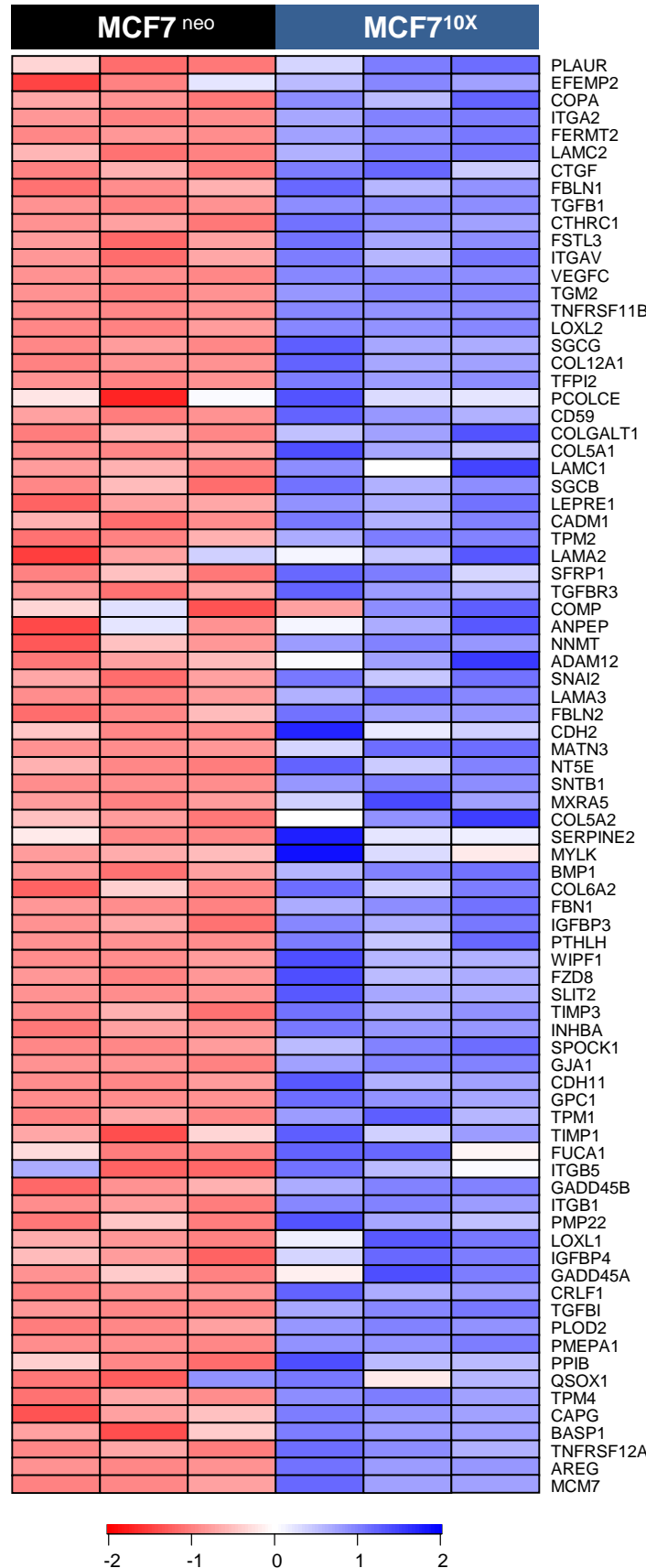
HALLMARK REACTIVE OXYGEN SPECIES PATHWAY



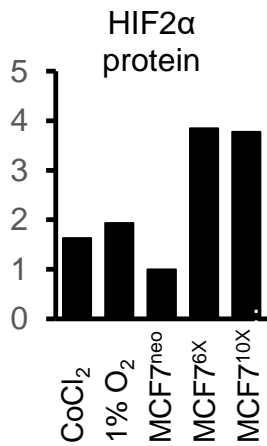
HALLMARK HYPOXIA



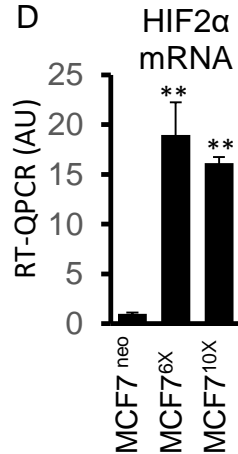
HALLMARK_EPITHELIAL_MESENCHYMAL_TRANSITION



B



D



C

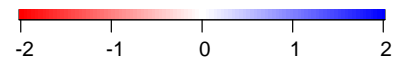
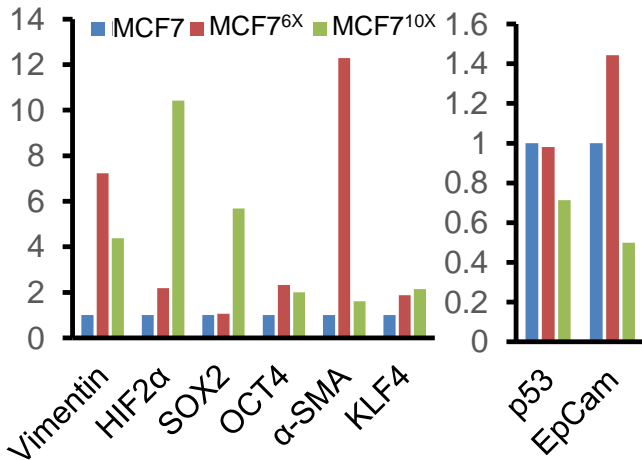
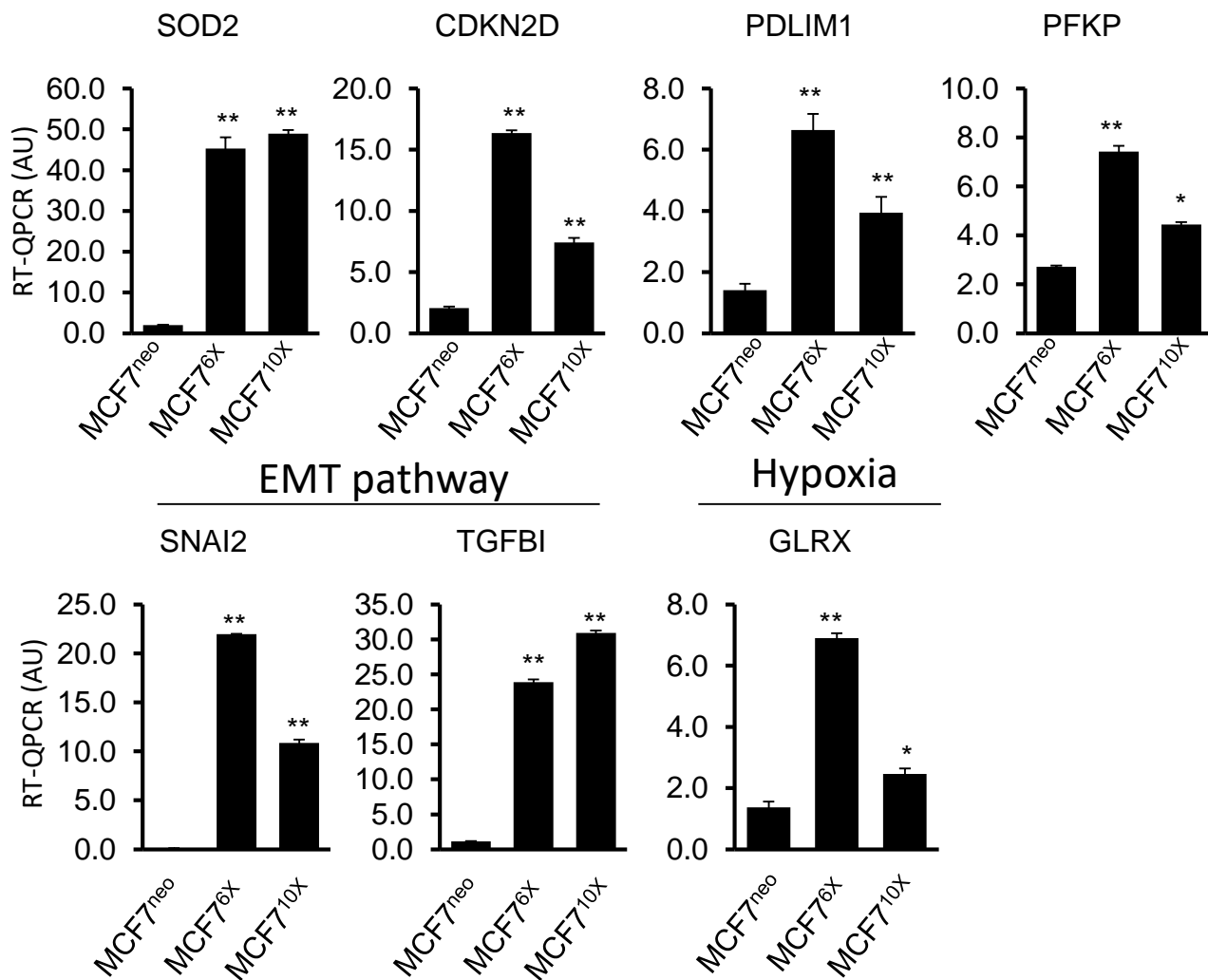


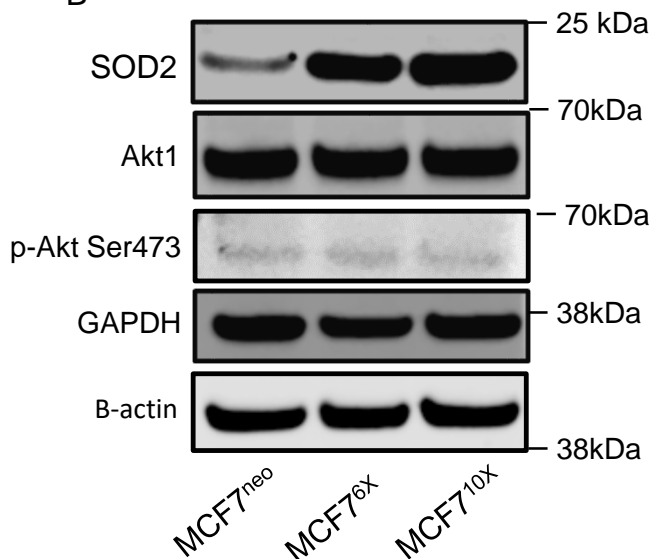
Figure S1

A

ROS pathway



B



C

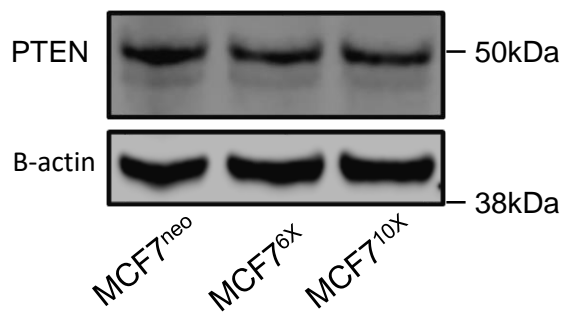


Figure S2

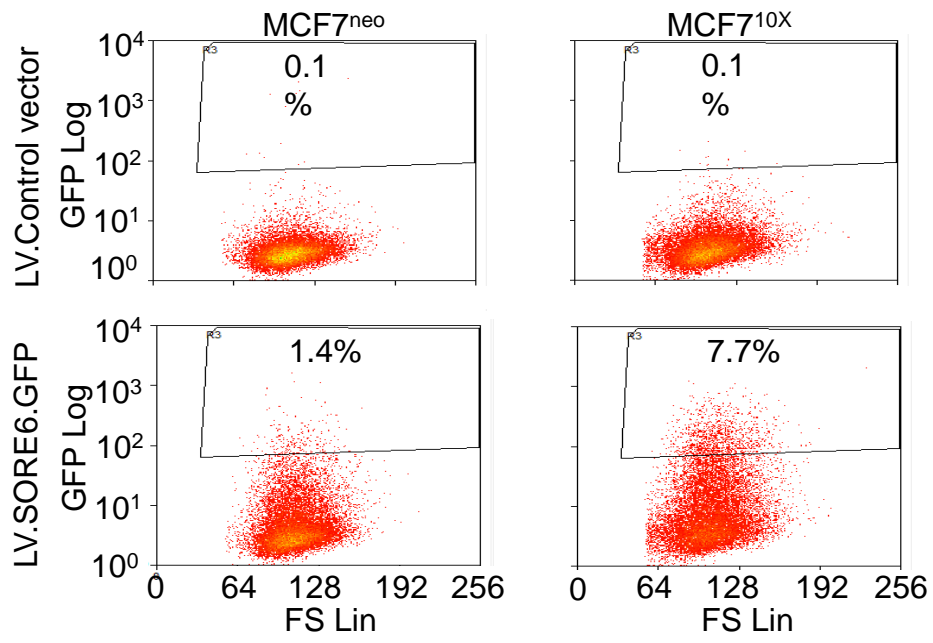


Figure S3

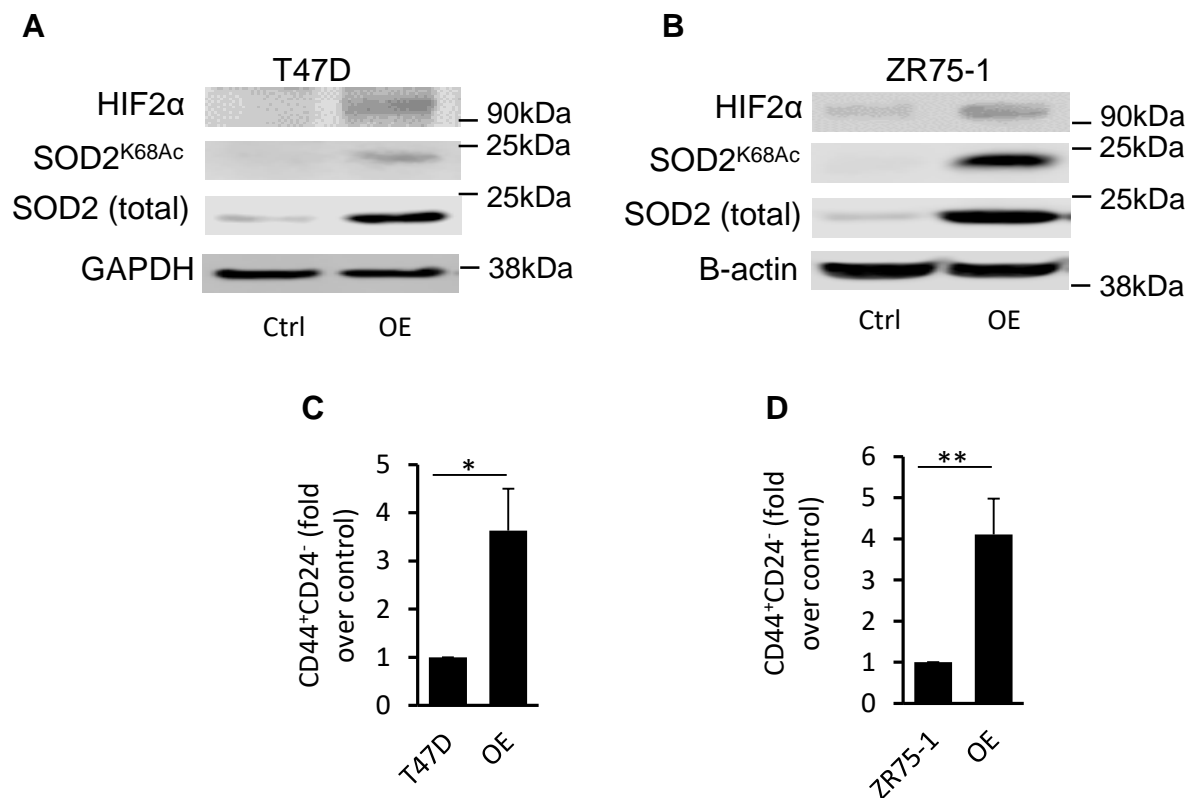
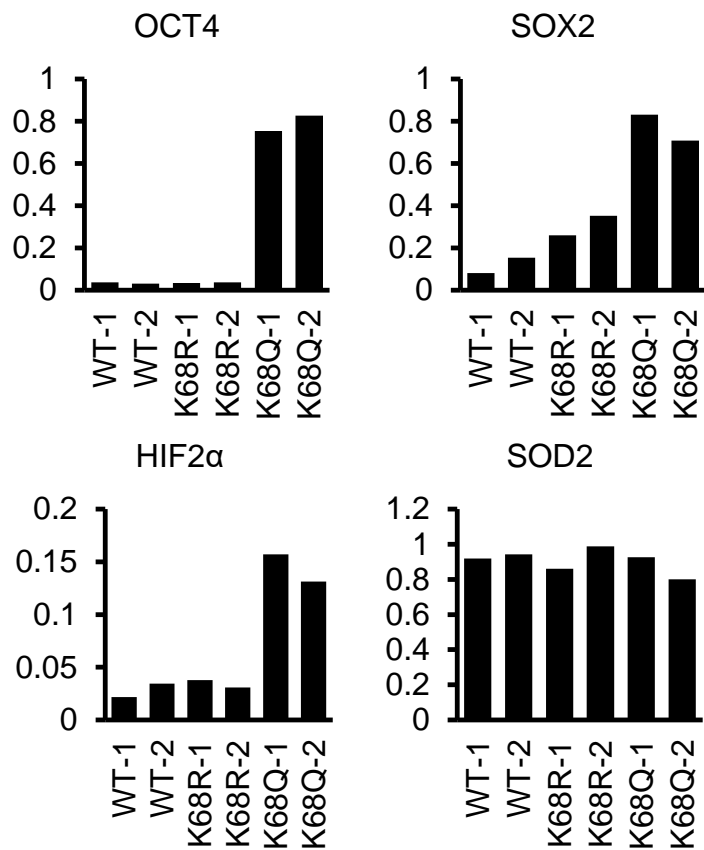
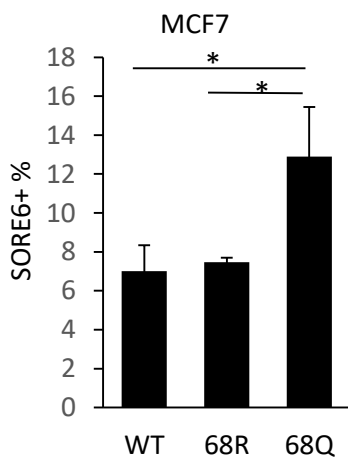
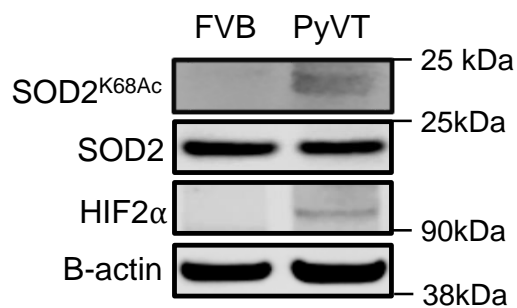


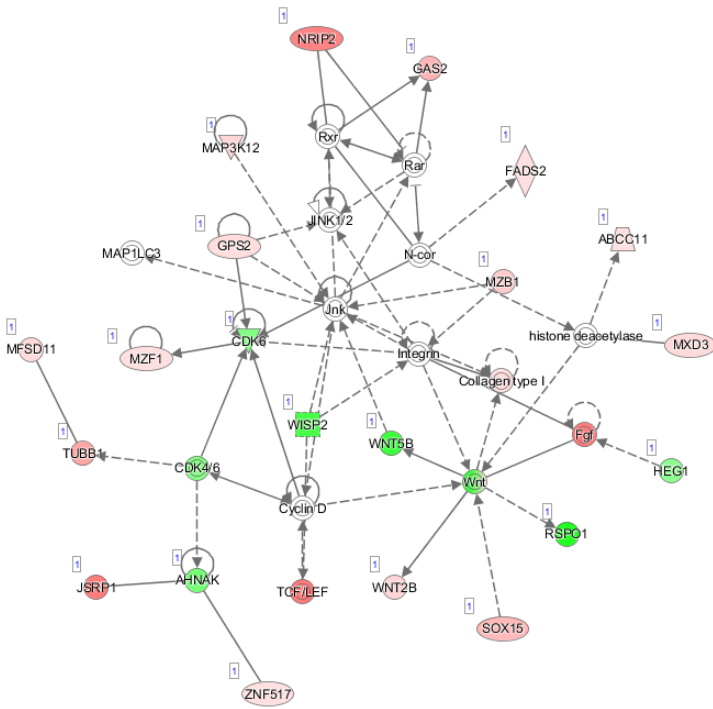
Figure S4

A**B**

*P<0.05, N=3

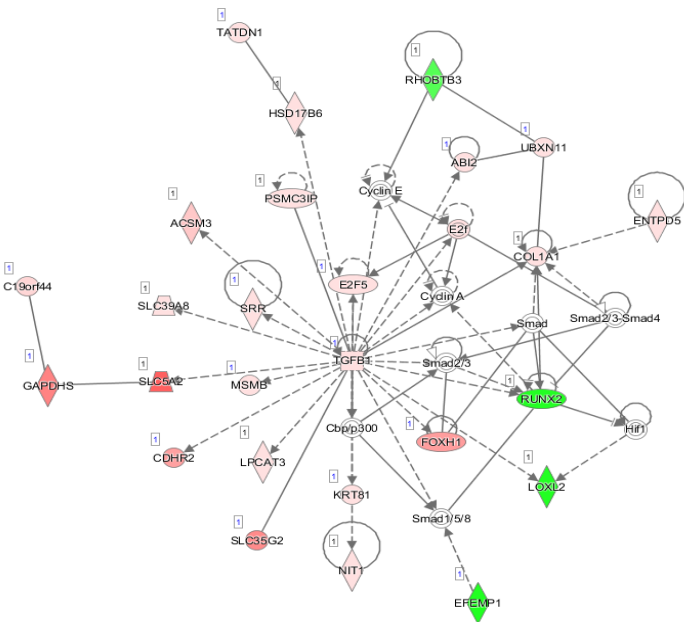
C**Figure S5**

Cancer



ABCC11 ↑	AHNAK ↓	CDK4/6	CDK6 ↓
Collagen type I	Cyclin D	FADS2 ↑	Fgf
GAS2 ↑	GPS2 ↑	HEG1 ↓	histone deacetylase
Integrin	JNK1/2	Jnk	JSRP1 ↑
MAP1LC3	MAP3K12 ↑	MZB1 ↑	MXD3 ↑
MZB1 ↑	MZF1 ↑	N-corr	NRIP2 ↑
Rar	RSP01 ↓	Ror	SOX15 ↑
TCF/LEF	TUBB1 ↑	WISP2 ↓	Wnt
WNT2B ↑	WNT5B ↓	ZNF517 ↑	

Cellular development



ABI2 ↑	ACSM3 ↑	C19orf44 ↑	Cbp/p300
CDHR2 ↑	COL1A1 ↑	Cyclin A	Cyclin E
E2f	E2F5 ↑	EFEMP1 ↓	ENTPD5 ↑
FOXH1 ↑	GAPDH5 ↑	Hf1	HSD17B6 ↑
KRT81 ↑	LOXL2 ↓	LPCAT3 ↑	MSMB ↑
NIT1 ↑	PSMC3IP ↑	RHOBTB3 ↓	RUNX2 ↓
SLC35G2 ↑	SLC39A8 ↑	SLC5A2 ↑	Smad
Smad1/5/8	Smad2/3	Smad2/3-Smad4	SRR ↑
TATDN1 ↑	TGFβ1 ↑	UBXL11 ↑	

Figure S6

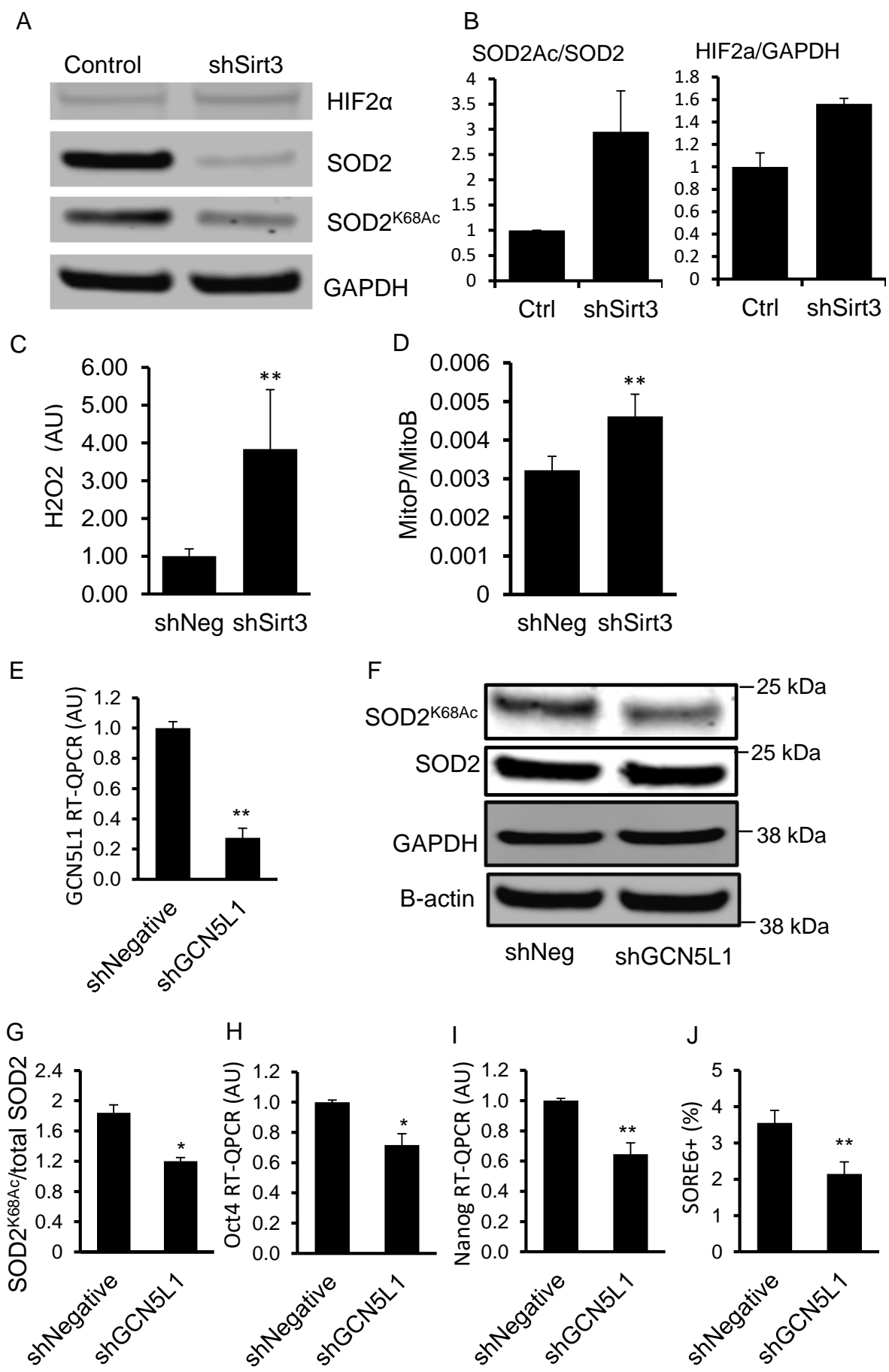


Figure S7

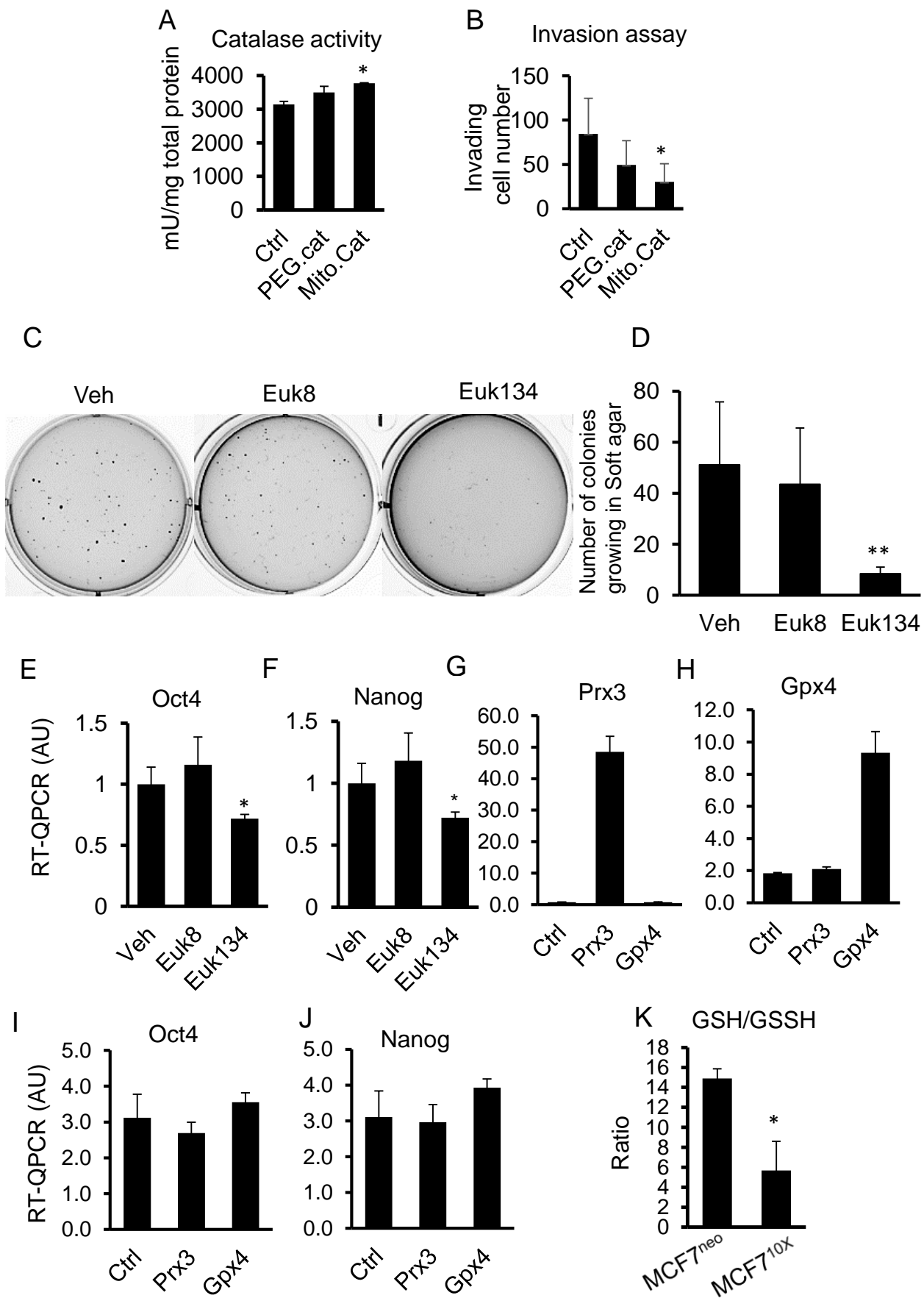


Figure S8